

## Research Article

**Non-Linear Mixed-Oberbeck Electroconvection in a Poorly Conducting Fluid Through a Vertical Channel in the Presence of Electric Field**Shashikala.B.S<sup>\*a</sup> and N. Rudraiah<sup>b</sup><sup>a</sup>Department of Mathematics, Govt. S.K.S.J.T.I, K.R.Circle,Bangalore-01<sup>b</sup>Centre for Advanced Studies in Fluid Mechanics, Department of Mathematics, Bangalore University, Bangalore-560 001**Abstract**

*Nonlinear Mixed –Oberbeck electroconvection in a poorly conducting fluid in a vertical channel in the presence of an electric field, viscous and Ohmic dissipations is investigated. The flow is governed by the modified Navier-Stokes and energy equations with boundaries which are kept at different temperatures. The nonlinear coupled momentum and energy equations are solved numerically using finite difference technique and analytically using regular perturbation method with  $B$ , as the perturbation parameter. The velocity and temperature fields are obtained for various values of electric number, Brinkman number and GR which is nothing but the ratio of Grashof number to the Reynolds number. We note that, if  $GR=0$ , the problem reduces to the forced convection. We have computed the local Nusselt number at the walls, the skin friction and mass flow rate. The analytical solutions are compared with those obtained from the numerical solution and good agreement is found. We found the effect of increase in the temperature difference between the plates is to increase the velocity and temperature distributions due to increase in convection. These results are useful in the effective control of heat transfer in many industrial problems.*

**Keywords:** Mixed Oberbeck Convection, Poorly Conducting Fluid, Skin friction, Heat transfer, Mass flow rate, Nusselt Number, Grashof Number, Brinkmann Number, Perturbation method and Electric Field.

**1. Introduction**

The study of combined free and forced convection called mixed convection(MC) in a vertical channel has received considerable attention because of its wide range of applications from cooling of electronic devices ,gas-cooled nuclear reactors to that of solar energy collectors. A comprehensive review on mixed convection can be found in [1] and [2]. One of the earliest study on laminar, fully developed mixed convection in a vertical channel with uniform wall temperature was by Tao[3]. Recently, Aung and Worku, Cheng et al, have studied the mixed convection in a vertical channel with symmetric and asymmetric heating at the walls. These authors reported that the buoyancy force can cause flow reversal both for upward and downward flows. More recently Barlcua, has studied the fully developed MC flow in a vertical channel with viscous dissipation. An analytical solution is found by a perturbation method. In particular he has studied the, forced convective flow with viscous heating as the base heat transfer process while the effect of buoyancy is accounted for by expressing the fluid velocity and temperature as power series in the ratio between the Grashof number and Reynolds number. Aung and Worku,

discussed the theory of combined free and forced convection in a vertical channel with flow reversal conditions for both developing and fully developed flows. Rudraiah et al [8] have studied the effect of oscillatory flow on mixed convection in a vertical porous stratum.

In contrast to MC due to variation of density with temperature discussed above there is another type of MC arising in a poorly conducting alloys like nickel-titanium( $Ni-Ti$ ), aluminum oxides and so on in a vertical channel due to variation of electrical conductivity,  $\sigma$ , with temperature in the presence of an electric field,  $\vec{E}$ , called mixed electroconvection (MEC). The variations of  $\sigma$  with temperature releases the charges forming distribution of charge density,  $\rho_e$  (See). These charges in turn induces the electric field,  $\vec{E}_i$  called thermal or induced electric field.

In addition these may be an applied electric field,  $\vec{E}_a$ , due to embedded electrodes of different potentials at the boundaries (See Fig.1). The total electric field  $\vec{E}(= \vec{E}_i + \vec{E}_a)$  in a poorly conducting fluid produces a current which acts as sensing. In addition this  $\vec{E}$  together with  $\rho_e$  produces an electric force  $\rho_e \vec{E}$  which acts as

\*Corresponding author: **Shashikala.B.S**

actuation. These two properties are the two important properties required a material to be a smart material. Therefore MEC plays a significant role to synthesis smart materials like shape memory alloys(SMA).These smart materials demonstrate great potential for enhancing the functionality, serviceability and durability of civil, mechanical, electrical and electronic infrastructure systems. In spite of these importance much attention has not been given to the study of MEC in a vertical channel. The study of it in the presence of total electric field, viscous and Joulean dissipations is the objective of this paper.

To achieve this objective we first obtain the modified conservation of momentum, energy together with Maxwell equations and continuity of charges, suitable for a poorly conducting mixed oberbeck electro convection. Modified in the sense of considering electric force in the momentum equation and ohmic dissipation in the energy equation.

**2 Mathematical Formulation**

Consider a steady, laminar, fully developed mixed convective flow in an open-ended vertical parallel plate channel filled with poorly conducting fluid. The Oberbeck-Boussinesq approximation is assumed to be valid following Rajagopal et al (1996). In other words we consider Oberbeck-Boussinesq, homogeneous, poorly conducting fluid, together with electrohydrodynamic (EHD) approximations(See Rudraiah et al,1996), namely  $\sigma$  is very small and hence induced magnetic field is negligible and there is no applied magnetic field.

It is assumed that the thermal conductivity, the dynamic viscosity and the thermal expansion coefficient are considered constant. The X-axis is chosen parallel to the gravitational field, but with opposite direction and Y-axis is transverse to the plates. The origin is such that the channel walls are at positions Y=0 and Y=2L, respectively as shown in figure 1.

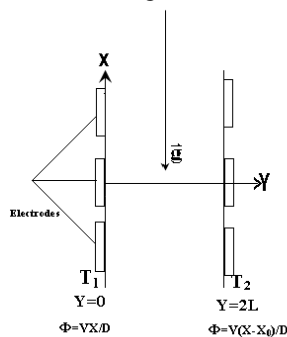


**Fig 1:** Physical Configuration

By the conduction of fully developed flow, the mass balance equation will be

$$\frac{\partial U}{\partial X} = 0$$

,so that U depends only on Y, where u is the velocity along the X-axis.

Then the required basic equations for steady flow are

$$g\beta(T-T_0) - \frac{1}{\rho_0} \frac{\partial P}{\partial X} + \frac{\mu}{\rho_0} \frac{d^2 U}{dY^2} + \frac{\rho_e E_x}{\rho_0} = 0 \tag{2.1}$$

$$\chi \frac{d^2 T}{dY^2} + \frac{\mu}{(\rho c_p)_f} \left( \frac{dU}{dY} \right)^2 + \frac{\sigma |\vec{E}|^2}{(\rho c_p)_f} = 0 \tag{2.2}$$

$$\sigma \left( \frac{d^2 \phi}{dX^2} + \frac{d^2 \phi}{dY^2} \right) + \frac{d\phi}{dY} \cdot \frac{d\sigma}{dY} = 0 \tag{2.3}$$

and the Maxwell equations for a poorly conducting fluid are

$$\nabla \cdot \vec{E} = \frac{\rho_e}{\epsilon_0}, \quad \vec{E} = -\nabla \phi, \quad \vec{J} = \sigma \vec{E}, \quad \sigma = \sigma_0 [1 + \alpha_b (T - T_0)] \tag{2.4a,b,c,d}$$

$$\sigma = 1 + \alpha \theta_b \quad \text{Where} \quad \alpha = \alpha_b \Delta T, \tag{2.4e}$$

We assume that the temperature of the boundary at Y=0 is

$$T_1, \text{ while that at } Y=2L \text{ is } T_2 \text{ with } T_2 \geq T_1 \text{ and } \frac{dP}{dX} \text{ is independent of } X. \text{ Let there exist a constant } A \text{ such that}$$

$$\frac{dP}{dX} = A \tag{2.5}$$

Evaluating the derivative of equation (2.1) with respect to X and using equation (2.5), we obtain

$$\frac{dT}{dX} = 0 \tag{2.6}$$

This implies that the temperature also depends only on the variable Y. The energy balance equation includes the effects of viscous and ohmic dissipations.

Equation (2.1), using (2.2) and (2.5), becomes

$$\frac{d^4 U}{dY^4} - \frac{g\beta}{\chi (c_p)_f} \left( \frac{dU}{dY} \right)^2 - \frac{g\beta}{\nu K} \sigma |\vec{E}|^2 + \frac{1}{\mu} \frac{d^2}{dY^2} (\rho_e E_x) = 0 \tag{2.7}$$

**3 Boundary Conditions**

The no-slip boundary conditions on U are

$$U(0) = U(2L) = 0 \tag{3.1}$$

$$T = T_1 \text{ at } Y = 0$$

$$T = T_2 \text{ at } Y = 2L \tag{3.2}$$

Using Equations (2.1) and (2.4), and using the boundary conditions on T we obtain

$$\left( \frac{d^2 U}{dY^2} \right)_{Y=0} = \frac{A}{\mu} - \frac{g\beta(T_1 - T_0)}{\nu} - \frac{\rho_e E_x}{\mu} \tag{3.3a}$$

$$\left( \frac{d^2 U}{dY^2} \right)_{Y=2L} = \frac{A}{\mu} - \frac{g\beta(T_2 - T_0)}{\nu} - \frac{\rho_e E_x}{\mu} \tag{3.3b}$$

$$\phi = VX/D \text{ at } Y = 0$$

$$\phi = V(X - X_0)/D \text{ at } Y = 2L \tag{3.4}$$

Equations (2.1)-(2.4) and (3.1)-(3.4) can be written in a dimensionless form by employing the dimensionless quantities

$$u^* = \frac{U}{U_0}, \theta = \frac{T - T_0}{\Delta T}, y^* = \frac{Y}{D}, E^* = \frac{E}{V/D}, x^* = \frac{X}{D}, \rho_e^* = \frac{\rho_e}{\epsilon_0 V/D^2}, \phi^* = \frac{\phi}{V}, \tag{3.5}$$

where D=2L is the hydraulic diameter. The reference velocity U<sub>0</sub> and the reference temperature T<sub>0</sub> are given by

$$U_0 = -\frac{AD^2}{48\mu}; \quad T_0 = \frac{T_1+T_2}{2} \quad (3.6)$$

The physical meanings of other quantities defined in (6.3.5) are explained in the earlier chapters. Moreover, the reference temperature difference  $\Delta T$  is given by

$$\Delta T = T_2 - T_1 \quad \text{if } T_1 < T_2 \quad (3.7)$$

Using (3.5), equations (2.1)-(2.4) and (3.1)-(3.4) become,

$$\frac{d^2\theta}{dy^2} + Br \left( \frac{du}{dy} \right)^2 + T_e \sigma [E_x^2 + E_y^2] = 0 \quad (3.8)$$

$$\frac{d^4u}{dy^4} - GR Br \left( \frac{du}{dy} \right)^2 - GR T_e \sigma [E_x^2 + E_y^2] + W_e \frac{d^2}{dy^2} (\rho_e E_x) = 0 \quad (3.9)$$

$$\sigma \left( \frac{d^2\phi}{dx^2} + \frac{d^2\phi}{dy^2} \right) + \frac{d\phi}{dy} \cdot \frac{d\sigma}{dy} = 0 \quad (3.10)$$

$$\nabla \cdot \vec{E} = \rho_e, \quad \sigma = 1 + \alpha\theta \quad \text{Where } \alpha = \alpha_b \Delta T, \quad (3.11)$$

$$u(0) = u(1) = 0 \quad (3.12)$$

$$\theta = -1/2 \quad \text{at } y=0$$

$$\theta = 1/2 \quad \text{at } y=1 \quad (3.13)$$

$$\left( \frac{d^2u}{dy^2} \right)_{y=0} = -48 + \frac{GR}{2} - W_1 \quad (3.14)$$

$$\left( \frac{d^2u}{dy^2} \right)_{y=1} = -48 - \frac{GR}{2} - W_1 e^{-\alpha} \quad (3.15)$$

$$\phi = x \quad \text{at } y=0$$

$$\phi = (x - x_0) \quad \text{at } y=1 \quad (3.16)$$

Further (2.1) using scales (3.5) and (3.6) can be written as

$$\frac{d^2u}{dy^2} + GR\theta + W_e (\rho_e E_x) + 48 = 0 \quad (3.17)$$

Rearranging (3.17), we get

$$\theta = -\frac{1}{GR} \left( 48 + \frac{d^2u}{dy^2} \right) - \frac{W_e}{GR} (\rho_e E_x) \quad (3.18)$$

where

$$Gr = \frac{g\beta\Delta TD^3}{\nu^2}, R_e = \frac{U_0 D}{\nu}, Br = \frac{\mu U_0^2}{K\Delta T}, GR = \frac{Gr}{Re}, W_e = \frac{\varepsilon_0 V^2}{\rho_0 g \beta \Delta T D^3}$$

#### 4 Solution for $\phi$ :

The solution for  $\phi$ , according to (3.10), depends on  $\sigma$  which in turn depends on the temperature  $\theta$  as in (3.11). In a poorly conducting fluid (i.e.,  $\sigma \ll 1$ ), the dissipations in (2.2) are negligible and hence  $\sigma$  will depend on the

conduction temperature,  $\theta_B$ , satisfying

$$\frac{d^2\theta_B}{dy^2} = 0 \quad (4.1)$$

The solution of this satisfying the boundary conditions

$$\theta_B = -1/2 \quad \text{at } y=0 \quad \text{and } \theta_B = 1/2 \quad \text{at } y=1 \quad (4.2)$$

$$\text{is } \theta_B = y - 1/2 \quad (4.3)$$

Then (3.11) becomes

$$\sigma = 1 + \alpha(y - 1/2) \approx e^{\alpha(y-1/2)} \quad (\because \alpha \ll 1) \quad (4.4)$$

Then (3.11) using (4.4) becomes

$$\frac{\partial^2\phi}{\partial x^2} + \frac{\partial^2\phi}{\partial y^2} + \alpha \frac{\partial\phi}{\partial y} = 0 \quad (4.5)$$

To find the solution of (4.5), as in the previous chapters, we consider the following two cases

#### Case 1: The Potential Difference Applied Opposite to the Temperature Difference

The solution of (4.5), satisfying (3.16), is

$$\phi = x - \frac{x_0}{(1-e^{-\alpha})} (1-e^{-\alpha y}) \quad (4.6)$$

From (2.4a, b, c, d), after making dimensionless using the quantities defined earlier and using (4.6), we get

$$\rho_e = \nabla \cdot \vec{E} = -\nabla^2\phi = -\frac{\alpha^2 x_0}{(1-e^{-\alpha})} e^{-\alpha y}, \quad E_x = -1, \quad E_y = \frac{\alpha x_0}{(1-e^{-\alpha})} e^{-\alpha y} \quad (4.7)$$

$$\rho_e E_x = \frac{\alpha^2 x_0}{(1-e^{-\alpha})} e^{-\alpha y}, \quad E_x^2 + E_y^2 = 1 + \frac{x_0^2 \alpha^2 e^{-2\alpha y}}{(1-e^{-\alpha})^2} \quad (4.8)$$

#### Case 2: The Potential Difference Applied in the Same Direction of Temperature Difference

In this case the boundary conditions on  $\phi$ , in dimensionless form, are opposite to those specified in (3.16) and they are

$$\phi = x \quad \text{at } y=1 \quad \text{and } \phi = x - x_0 \quad \text{at } y=0 \quad (4.9)$$

In this case the solution of (4.5), satisfying (4.9), is

$$\phi = x + \frac{x_0}{(1-e^{-\alpha})} (e^{-\alpha} - e^{-\alpha y}) \quad (4.10)$$

We note that  $\rho_e$ ,  $E_y$  and  $\rho_e E_x$  are opposite to those obtained in case 1, where as  $E_x$  and  $E_x^2 + E_y^2$  remain the same as in case 1.

### 5 Analytical Solution

Since (3.8) and (3.17) are coupled equations, we find the solutions of these equations analytically using perturbation technique with Brinkman number (Br) as the perturbation parameter, using the boundary conditions given in (3.12) and (3.13) for different temperature combinations mentioned below. Another way of finding the solution of the problem is to use (3.9) along with the boundary conditions (3.12), (3.14) and (3.15). We observe that in both the cases, we will get the same values. In this section we find the solution below following the first method. We obtain that, when the buoyancy forces are dominating i.e., when  $GR \rightarrow \pm\infty$ , in the case of asymmetric heating, it is purely natural convection. On the other hand, when buoyancy forces are negligible and viscous dissipation is dominating, i.e.,  $GR=0$ , a purely forced convection occurs. The solution of (3.8) and (3.17) for a fixed value of  $GR \neq 0$  is obtained, for small values of  $Br$ , using the series

$$u(y) = u_0(y) + Br u_1(y) + Br^2 u_2(y) + \dots = \sum_{n=0}^{\infty} Br^n u_n(y) \quad (5.1)$$

$$\theta(y) = \theta_0(y) + Br \theta_1(y) + Br^2 \theta_2(y) + \dots = \sum_{n=0}^{\infty} Br^n \theta_n(y) \quad (5.2)$$

Case 1: Isothermal-Isothermal Walls

Substituting (5.1) and (5.2) in (3.8) and (3.17), we get

$$\frac{d^2\theta}{dy^2} + B_r \left(\frac{du}{dy}\right)^2 + T_e e^{-\alpha/2} e^{\alpha y} + W_2 e^{-\alpha y} = 0 \tag{5.3}$$

$$\frac{d^2u}{dy^2} + GR\theta + W_1 e^{-\alpha y} + 48 = 0 \tag{5.4}$$

Substituting series (5.1) and (5.2) in to (5.3), (5.4) and equating coefficients of like powers of  $B_r$  to zero, we obtain the boundary value problem for  $n=0$  and 1 as

$$\frac{d^2u_0}{dy^2} + GR\theta_0 + W_1 e^{-\alpha y} + 48 = 0 \tag{5.5}$$

$$\frac{d^2\theta_0}{dy^2} + T_e e^{-\alpha/2} e^{\alpha y} + W_2 e^{-\alpha y} = 0 \tag{5.6}$$

$$\frac{d^2u_1}{dy^2} + GR\theta_1 = 0 \tag{5.7}$$

$$\frac{d^2\theta_1}{dy^2} + B_r \left(\frac{du_0}{dy}\right)^2 = 0 \tag{5.8}$$

$$u_0(0) = u_0(1) = 0 \tag{5.9}$$

$$u_1(0) = u_1(1) = 0 \tag{5.10}$$

$$\theta_0 = -1/2 \text{ at } y=0 \text{ and } \theta_0 = 1/2 \text{ at } y=1 \tag{5.11}$$

$$\theta_1 = 0 \text{ at } y=0 \text{ and } 1 \tag{5.12}$$

Solving (6.5.5) to (6.5.8) using (6.5.9) to (6.5.12), we get

$$\theta_0 = -W_2 (e^{-\alpha} - e^{-\alpha y} - 1) + T_e e^{-\alpha/2} (e^{\alpha} - e^{-\alpha y} - 1) + \alpha^2 y \tag{5.13}$$

$$u_0 = \frac{a_1}{\alpha^2} (y + e^{-\alpha y} - e^{-\alpha} - 1) + \frac{a_2}{\alpha^2} (y + e^{\alpha y} - e^{\alpha} - 1) + \frac{GRC_1}{6} + \frac{a_3}{2} (1 - y^2) \tag{5.14}$$

$$\theta_1 = -\left(\frac{a_1^2 e^{-2\alpha y} + a_2^2 e^{2\alpha y}}{4\alpha^4}\right) + y^2 \left(\frac{a_2 GRC_1 e^{\alpha y} - a_1 GRC_1 e^{-\alpha y}}{\alpha^3}\right) + (a_{12} e^{\alpha y} + a_{13} e^{-\alpha y}) \tag{6.5.15}$$

$$+ y \left( C_5 + \frac{a_5}{2} y - \frac{a_3 C_3}{3} y^2 + \frac{a_4}{4} y^3 + \frac{GRC_1 a_3}{20} y^4 - \frac{GRC_1^2}{120} y^5 + a_{10} e^{\alpha y} + a_{11} e^{-\alpha y} \right) + C_6$$

$$+ y^2 \left( a_{18} e^{-2\alpha y} + a_{19} e^{2\alpha y} \right) + y \left( a_{27} e^{\alpha y} + a_{28} e^{-\alpha y} + C_7 \right) + \left( a_{29} e^{\alpha y} + a_{30} e^{-\alpha y} \right) + C_8 \tag{5.16}$$

Here,  $W_i (i = 1 \text{ to } 2), C_i (i = 1 \text{ to } 8), a_i (i = 1 \text{ to } 30)$ ,

$$W_1 = \frac{W_e x_0 \alpha^2}{(1 - e^{-\alpha})}, \quad W_2 = \frac{T_e x_0^2 \alpha^2 e^{-\alpha/2}}{4(1 - e^{-\alpha})^2}$$

are constants.

Case2: Isothermal-Isoflux Walls

The Isoflux and Isothermal boundary conditions for the channel walls are given by

$$q_1 = K \left(\frac{dT}{dY}\right)_{Y=0}; \quad T(2L) = T_2 \tag{5.17}$$

In the non-dimensional form of (5.17), using (3.5) with  $\Delta T = \frac{q_1 D}{K}$ , becomes

$$\left(\frac{d\theta}{dY}\right)_{y=0} = 1; \quad \theta(1) = \theta_2 \tag{5.18}$$

where  $\theta_2 = \frac{T_2 - T_0}{\Delta T}$  is the thermal ratio parameter

$$\text{Using (5.18) in (4.1) we get } \sigma = 1 + \alpha (y + \Omega) \approx e^{\alpha(y+\Omega)} \tag{5.19}$$

where  $\Omega = \theta_2 - 1$

$$\text{Using this, we get } \phi = x - \frac{x_0}{(1 - e^{-\alpha})} (1 - e^{-\alpha y}) \tag{5.20}$$

From (5.20) we obtain  $\rho_e E_x, E_x, E_y$ . Following the above procedure, (3.8) and (3.17) take the form

$$\frac{d^2u}{dy^2} + GR\theta + W_1 e^{-\alpha y} + 48 = 0 \tag{5.21}$$

$$\frac{d^2\theta}{dy^2} + B_r \left(\frac{du}{dy}\right)^2 + T_e e^{\alpha\Omega} e^{\alpha y} + W_4 e^{-\alpha y} = 0 \tag{5.22}$$

Substituting series (5.1) and (5.2) in to (5.21) and (5.22) and equating coefficients of like powers of  $B_r$  to zero, we obtain the boundary value problem for  $n=0$  and 1 as

$$\frac{d^2u_0}{dy^2} + GR\theta_0 + W_1 e^{-\alpha y} + 48 = 0 \tag{5.23}$$

$$\frac{d^2\theta_0}{dy^2} + T_e e^{\alpha\Omega} e^{\alpha y} + W_4 e^{-\alpha y} = 0 \tag{5.24}$$

$$\frac{d^2u_1}{dy^2} + GR\theta_1 = 0 \tag{5.25}$$

$$\frac{d^2\theta_1}{dy^2} + B_r \left(\frac{du_0}{dy}\right)^2 = 0 \tag{5.26}$$

$$u_0(0) = u_0(1) = 0 \tag{5.27}$$

$$u_1(0) = u_1(1) = 0 \tag{5.28}$$

$$\left(\frac{d\theta_0}{dy}\right)_{y=0} = 1 \text{ and } \theta_0 = 1/2 \text{ at } y=1 \tag{5.29}$$

$$\left(\frac{d\theta_1}{dy}\right)_{y=0} = 0 \text{ and } \theta_1 = 0 \text{ at } y=1 \tag{5.30}$$

Solving (5.23) to (5.26) using (5.27) to (5.30), we get

$$\theta_0 = 2T_e e^{\alpha\Omega} (e^{\alpha} - e^{\alpha y} + \alpha(y-1)) + 2W_4 (e^{-\alpha} - e^{-\alpha y} + \alpha(1-y)) + \alpha^2 (2y-1) \tag{5.31}$$

$$u_0 = \frac{a_1}{\alpha^2} (y + e^{-\alpha y} - e^{-\alpha} - 1) + \frac{a_2}{\alpha^2} (y + e^{\alpha y} - e^{\alpha} - 1) + \frac{GRC_1}{6} + \frac{a_3}{2} (1 - y^2) \tag{5.32}$$

$$\theta_1 = -\left(\frac{a_1^2 e^{-2\alpha y} + a_2^2 e^{2\alpha y}}{4\alpha^4}\right) + y \left( a_{10} e^{\alpha y} + a_{11} e^{-\alpha y} + C_5 \right) + \left( a_{12} e^{\alpha y} + a_{13} e^{-\alpha y} + C_6 \right) \tag{5.33}$$

$$+ y^2 \left( \frac{a_2 GRC_1 e^{\alpha y} - a_1 GRC_1 e^{-\alpha y} + \frac{a_5}{2} - \frac{a_3 C_3}{3} y + \frac{a_4}{4} + \frac{GRC_1 a_3}{20} y^3 - \frac{GRC_1^2}{120} y^4 \right) \tag{5.34}$$

$$+ y \left( a_{18} e^{-2\alpha y} + a_{19} e^{2\alpha y} \right) + \left( a_{29} e^{\alpha y} + a_{30} e^{-\alpha y} \right) + y \left( -\frac{C_5 GR}{6} y^2 - \frac{GRC_6}{2} y + C_7 \right) + y^2 \left( a_{25} e^{\alpha y} + a_{26} e^{-\alpha y} + a_{24} y^2 + a_{23} y^3 + a_{22} y^4 + a_{21} y^5 + a_{20} y^6 \right) + C_8$$

Where  $W_i (i = 1, 4), C_i (i = 1 \text{ to } 8), a_i (i = 1 \text{ to } 30)$ ,

$$W_4 = \frac{T_e x_0^2 \alpha^2 e^{\alpha\Omega}}{4(1 - e^{-\alpha})^2}$$

are constants.

Case3: Isoflux-Isoflux Walls

The Isoflux and Isoflux boundary conditions for the channel walls are given by

$$q_1 = K \left( \frac{dT}{dY} \right)_{Y=0} ; \quad q_2 = K \left( \frac{dT}{dY} \right)_{Y=1} \tag{5.35}$$

In the non-dimensional form of (5.35), using (3.5) with

$$\Delta T = \frac{q_1 D}{K}, \text{ becomes } \left( \frac{d\theta}{dY} \right)_{Y=0} = 1 ; \left( \frac{d\theta}{dY} \right)_{Y=1} = \lambda_1 \tag{5.36}$$

In addition to this we use the boundary condition is

$$\int_0^1 \theta dy = Q \tag{5.37}$$

$$\lambda_1 = \frac{q_2}{q_1}$$

where  $q_1$  is the ratio of heat fluxes.

Using (5.36) and (5.37) in (4.1) and then from (3.11) we get

$$\sigma = 1 + \alpha (\lambda_1 y + \Omega_1) \approx e^{\alpha(\lambda_1 y + \Omega_1)} \tag{5.38}$$

Using this in (3.10) and then solving using (3.16), we get

$$\phi = x - \frac{x_0}{(1 - e^{-\alpha_1})} (1 - e^{-\alpha_1 y}) \tag{5.39}$$

where  $\Omega_1 = Q - \frac{\lambda_1}{2}, \alpha_1 = \alpha \lambda_1$  is constant.

From (5.39) we obtain  $\rho_e E_x, E_x, E_y$ .

Following the above procedure, we get the following equations

$$\frac{d^2 u_0}{dy^2} + GR\theta_0 + W_1 e^{-\alpha_1 y} + 48 = 0 \tag{5.40}$$

$$\frac{d^2 \theta}{dy^2} + B_r \left( \frac{du}{dy} \right)^2 + T_e e^{\alpha \Omega_1} e^{\alpha_1 y} + W_3 e^{-\alpha_1 y} = 0 \tag{5.41}$$

Substituting series (5.1) and (5.2) in to (5.40) and (5.41) and equating coefficients of like powers of  $B_r$  to zero, one obtains the boundary value problem for  $n=0$  and 1 as

$$\frac{d^2 u_0}{dy^2} + GR\theta_0 + W_1 e^{-\alpha_1 y} + 48 = 0 \tag{5.42}$$

$$\frac{d^2 \theta_0}{dy^2} + T_e e^{\alpha \Omega_1} e^{\alpha_1 y} + W_3 e^{-\alpha_1 y} = 0 \tag{5.43}$$

$$\frac{d^2 u_1}{dy^2} + GR\theta_1 = 0 \tag{5.44}$$

$$\frac{d^2 \theta_1}{dy^2} + B_r \left( \frac{du_0}{dy} \right)^2 = 0 \tag{5.45}$$

$$u_0(0) = u_0(1) = 0 \tag{5.46}$$

$$u_1(0) = u_1(1) = 0 \tag{5.47}$$

$$\left( \frac{d\theta_0}{dY} \right)_{Y=1} = \lambda_1 \text{ and } \int_0^1 \theta_0 dy = Q \tag{5.48}$$

$$\left( \frac{d\theta_1}{dY} \right)_{Y=1} = 0 \text{ and } \int_0^1 \theta_1 dy = 0 \tag{5.49}$$

Solving (5.42) to (5.45) using (5.46) to (5.49), we get

$$\theta_0 = \frac{T_e e^{\alpha \Omega_1}}{2\alpha_1^3} \left( 2e^{\alpha_1 y} \alpha_1 - e^{\alpha_1} \alpha_1^2 - 2e^{\alpha_1 y} \alpha_1 + 2(e^{\alpha_1} - 1) \right) + \frac{W_3}{2\alpha_1^3} \left( e^{\alpha_1} \alpha_1^2 - 2e^{\alpha_1 y} \alpha_1 - 2e^{\alpha_1} y \alpha_1 + 2W_3(1 - e^{-\alpha_1}) \right) + \frac{\lambda_1}{2} (2y - 1) + Q \tag{5.50}$$

$$u_0 = \frac{l_1}{\alpha_1^2} (y + e^{-\alpha_1 y} - e^{-\alpha_1} - 1) + \frac{l_2}{\alpha_1^2} (y + e^{\alpha_1 y} - e^{\alpha_1} - 1) + \frac{GRd_1}{6} + \frac{l_3}{2} (1 - y^2) \tag{5.51}$$

$$\theta_1 = - \left( \frac{l_1^2 e^{-2\alpha_1 y} + l_2^2 e^{2\alpha_1 y}}{4\alpha_1^4} \right) + y \left( l_{10} e^{-\alpha_1 y} + l_{11} e^{\alpha_1 y} + d_5 \right) + \left( l_{12} e^{-\alpha_1 y} + l_{13} e^{\alpha_1 y} + d_6 \right) + y^2 \left( \frac{l_5 GR d_1 e^{-\alpha_1 y} + l_4 GR d_1 e^{\alpha_1 y}}{\alpha_1^3} \right) + y^2 \left( \frac{l_4}{4} y^2 - \frac{l_3 d_3}{3} y + \frac{l_5}{2} + \frac{GR d_1 l_3}{20} y^3 + \frac{GR^2 d_1^2}{120} y^4 \right) \tag{5.52}$$

$$u_1 = \left( \frac{GR l_1^2 e^{2\alpha_1 y} + GR l_2^2 e^{-2\alpha_1 y}}{16\alpha_1^6} \right) + y^2 \left( \frac{l_2 GR^2 d_1 e^{-\alpha_1 y} - l_1 GR^2 d_1 e^{\alpha_1 y}}{\alpha_1^5} \right) + y \left( l_{22} e^{-\alpha_1 y} + l_{23} e^{\alpha_1 y} + d_7 - \frac{d_6 GR}{2} y \right) + \left( l_{24} e^{-\alpha_1 y} + l_{25} e^{\alpha_1 y} + d_8 \right) + y^3 \left( - \frac{d_5 GR}{6} - \frac{l_5 GR}{24} y + \frac{d_3 l_3 GR}{60} y^2 - \frac{l_4 GR}{120} y^3 - \frac{GR^2 d_1 l_3}{120 \cdot 7} y^4 + \frac{GR^3 d_1^2}{120 \cdot 56} y^4 \right) \tag{5.53}$$

where  $W_i (i = 1, 3), d_i (i = 1 \text{ to } 8), l_i (i = 1 \text{ to } 25)$ ,

$$W_3 = \frac{T_e x_0^2 \alpha_1^2 e^{\alpha \Omega_1}}{4(1 - e^{-\alpha_1})^2}$$

are constants.

## 6 Numerical Method

The analytical solutions obtained in Section 5 using regular perturbation technique are valid only for small values of the parameter  $B_r$ . However in many practical problems like unconventional generators, shock tubes, nuclear reactors and so on, the values of  $B_r$  are usually large and regular perturbation solutions cannot be used. For arbitrary values of  $B_r$ , analytical solutions for the nonlinear coupled equations derived in section 5 are complicated and hence as in the previous chapters, we resort to numerical solution using the finite difference technique. For numerical method, we consider the first case. The velocity and energy equations are solved using the central difference method. The use of central difference scheme replaces the derivative with the corresponding central difference approximations leading to the set of linear algebraic equations. The solutions of the reduced algebraic equations are obtained by the Method of Relaxation. The relaxation parameter  $\omega$  is fixed by comparing the numerical results with those obtained by analytical method. The convergence criterion is based on the step size and the previous iterations for the iterative difference to the order  $10^{-6}$ .

### 6.1 Isothermal-Isothermal Walls

The finite difference equations of (5.3) and (5.4) using central difference scheme with 21 mesh point with the step size (h) 0.05 are:

$$\frac{u_{j+1} - 2u_j + u_{j-1}}{h^2} + W_1 e^{-\alpha y_j} + GR\theta_j + 48 = 0 \tag{6.1.1}$$

Solving for  $u_j$

$$L_1 = \frac{1}{2} \left[ u_{j+1} + u_{j-1} + W_1 e^{-\alpha y_j} h^2 + GR\theta_j h^2 + 48h^2 \right] \tag{6.1.2}$$

Similarly,

$$\frac{\theta_{j+1} - 2\theta_j + \theta_{j-1}}{h^2} + Br \left( \frac{u_{j+1} - u_{j-1}}{2h} \right)^2 + T_e e^{-\alpha/2} e^{\alpha y_j} + W_2 e^{-\alpha y_j} = 0 \tag{6.1.3}$$

Solving for  $\theta_j$

$$L_2 = \frac{1}{2} \left[ \theta_{j+1} + \theta_{j-1} + \frac{Br}{4} (u_{j+1} - u_{j-1})^2 + T_e h^2 e^{-\alpha/2} e^{\alpha y_j} + W_2 h^2 e^{-\alpha y_j} \right] \tag{6.1.4}$$

where  $h = (\Delta y) = 0.05$  and  $j$  represents the mesh point and it varies from 0 to 20.

Equations (6.1.3) and (6.1.4) give two implicit equations in  $u_j$  and  $\theta_j$  denoted by  $L_1$  and  $L_2$  respectively. They separately generate systems of linear equations in  $u_j, u_{j+1}, u_{j-1}$  and  $\theta_j, \theta_{j+1}, \theta_{j-1}$ , resulting in tri-diagonal co-efficient matrices. These equations are solved using the Method of Relaxation.

*The Algorithm*

Initially we choose all  $u_j$  and  $\theta_j$  to be zero. This assumption is automatically corrected as the iteration proceeds. The Scheme of the Relaxation Method for the  $k^{th}$  iteration and  $j^{th}$  mesh point is:

$$u_j^k = \omega [u_j^k]_{L_1} + (1-\omega)u_j^{k-1} \quad \text{and} \quad \theta_j^k = \omega [\theta_j^k]_{L_2} + (1-\omega)\theta_j^{k-1}$$

Here  $\omega$  is the relaxation parameter. This translates into:

$$u_j^k = \omega \left[ \frac{1}{2} \left[ u_{j+1}^k + u_{j-1}^k + W_1 e^{-\alpha y_j} h^2 + GR\theta_j h^2 + 48h^2 \right] \right] + (1-\omega)u_j^{k-1} \tag{6.1.5}$$

and similarly for  $\theta$  we get:

$$\theta_j^k = \omega \left[ \frac{1}{2} \left[ \theta_{j+1}^k + \theta_{j-1}^k + \frac{Br}{4} (u_{j+1} - u_{j-1})^2 + h^2 T_e e^{-\alpha/2} e^{\alpha y_j} + W_2 h^2 e^{-\alpha y_j} \right] \right] + (1-\omega)\theta_j^{k-1} \tag{6.1.6}$$

where  $y_j = y_0 + jh$  with an initial guess and  $y_0 = 0$ .

The boundary conditions for  $u$ , given by  $u_{y=0} = 0$  and  $u_{y=1} = 0$ , are incorporated as:

$$u_0 = 0 \text{ and } u_{20} = 0$$

Similarly, we use  $\theta_{y=0} = -0.5$  and  $\theta_{y=1} = 0.5$ . That is  $\theta_0 = -0.5$  and  $\theta_{20} = 0.5$

Equations (6.1.5) and (6.1.6) are solved simultaneously from  $k=0$  at each mesh  $j$  point till the required order of iterative difference is achieved after comparison with the analytical results.

*6.2 Case2: Isothermal-Isoflux Walls*

Even in this case, applying the same procedures as described above to (5.21) and (.22), we get:

$$u_j^k = \omega \left[ \frac{1}{2} \left[ u_{j+1}^k + u_{j-1}^k + W_1 e^{-\alpha y_j} h^2 + GR\theta_j h^2 + 48h^2 \right] \right] + (1-\omega)u_j^{k-1} \tag{6.2.1}$$

The boundary conditions for  $u$  given by  $u_{y=0} = 0$  and  $u_{y=1} = 0$  are incorporated as:

$$u_0 = 0 \text{ and } u_{20} = 0.$$

Since we encounter a Neumann Boundary Condition at one wall for  $\theta$ , we have employed the Shooting Method to determine  $\theta_j$  from  $j=0$  to 20. The boundary conditions for  $\theta$  are given by  $\frac{d\theta}{dy}_{y=0} = 1$  and  $\theta_{y=1} = 0.5$ .

$$\frac{d\theta}{dy}_{y=0} = 1 \quad \text{and} \quad \theta_{y=1} = 0.5. \tag{6.2.2}$$

We define:  $\left( \frac{d\theta}{dy} \right)_j = t_j$ , and make an assumption  $\theta_0 = 1$ .  $\tag{6.2.3}$

Therefore (6.2.2) becomes

$$\left( \frac{dt}{dy} \right)_j + Br \left( \frac{u_{j+1} - u_{j-1}}{2h} \right)^2 + T_e e^{\alpha\Omega} e^{\alpha y_j} + W_4 e^{-\alpha y_j} = 0, \quad t_0 = 0 \tag{6.2.4}$$

Equations (6.2.3) and (6.2.4) convert the boundary value problem (5.22) into two initial value problems in  $\theta$  and  $t$  which are solved using the Euler's Method as given below:

$$\theta_j^k = \theta_{j-1}^k + h \left( \frac{d\theta}{dy} \right)_{j-1} \tag{6.2.5}$$

$$t_j^k = t_{j-1}^k + h \left( \frac{dt}{dy} \right)_{j-1} \tag{6.2.6}$$

Where  $\frac{d\theta}{dy}$  and  $\frac{dt}{dy}$  are given by (6.2.3) and (6.2.4) respectively. The equation (6.2.1) is separately solved at each mesh point  $j$  for  $k=0$ . Then equations (6.2.3)-(6.2.6) are solved simultaneously at each mesh point  $j$  for  $k=0$ .

This process is then iterated and in the end  $\theta_0$  is varied so that we get  $\theta_{y=1} = 0.5$ .

*6.3 Case3: Isoflux-Isoflux Walls*

Applying the same procedure described above to (5.40) we get:

$$u_j^k = \omega \left[ \frac{1}{2} \left[ u_{j+1}^k + u_{j-1}^k + W_1 e^{-\alpha y_j} h^2 + GR\theta_j h^2 + 48h^2 \right] \right] + (1-\omega)u_j^{k-1} \tag{6.3.3}$$

The boundary conditions for  $u$  given by  $u_{y=0} = 0$  and  $u_{y=1} = 0$  are incorporated as:

$$u_0 = 0 \text{ and } u_{20} = 0.$$

Since we encounter Neumann Boundary Condition at both the walls for  $\theta$ , we have employed the Shooting Method to determine  $\theta_j$  for  $j=0$  to 20. The boundary conditions for  $\theta$  given are given by  $\frac{d\theta}{dy}_{y=0} = 1$  and  $\frac{d\theta}{dy}_{y=1} = \lambda_1$ . Proceeding in the same way as described in Section 6.2, to (5.41) we get :

$$\left(\frac{d\theta}{dy}\right)_j = t_j, \text{ assuming } \theta_0 = 1. \tag{6.3.4}$$

$$\left(\frac{dt}{dy}\right)_j + Br \left(\frac{u_{j+1} - u_{j-1}}{2h}\right)^2 + T_e e^{\alpha \lambda_1} e^{\alpha y_j} + W_3 e^{-\alpha y_j} = 0, \quad t_0 = 0 \tag{6.3.5}$$

$$\theta_j^k = \theta_{j-1}^k + h \left(\frac{d\theta}{dy}\right)_{j-1} \tag{6.3.6}$$

$$t_j^k = t_{j-1}^k + h \left(\frac{dt}{dy}\right)_{j-1} \tag{6.3.7}$$

The above equations are solved as described in Section 6.2

and the value of  $\theta_0$  is varied so to get  $\left(\frac{d\theta}{dy}\right)_{y=1} = \lambda_1$ .

These solutions for  $u$  and  $\theta$  in each section are computed for different values of the parameters and the results are depicted graphically in figures (6.2) to (6.16) along with the analytical results and conclusions are drawn.

### 7 Skin friction, rate of heat transfer and mass flow rate

We found the Skin friction, Rate of heat transfer and Mass flow rate using the expressions after non dimensionless

$$\tau' = \mu(\partial U / \partial Y)_{Y=0,2L}, \quad q' = -K(\partial T / \partial y)_{y=0,2L},$$

$$m_E = \int_{-b}^b \rho_0 u dy$$

### 8. Results and discussions

The effect of electric field on the velocity, temperature, are obtained both analytically and numerically and the results are depicted in figures. The analytical solution for mixed convective poorly conducting fluid flow and heat transfer in a vertical channel is obtained using regular perturbation method. A numerical procedure is also performed to obtain the solutions in the presence of dissipative forces. The viscous and ohmic dissipations terms are included in the energy equation. The analytical solutions have been determined using  $Br$  as perturbation parameter. The heat transfer coefficient is obtained for three different thermal boundary conditions.

The velocity and temperature fields in the case of asymmetric heating are obtained and are depicted in figs 6.2a to 6.3b,(6.7a) to (6.8b) and(6.12a) to(6.13b).For asymmetric heating the temperature specified at the

boundaries are different and hence velocity and temperature fields depend on the perturbation parameter  $Br$ . Figs 6.2c, 6.7b ,6.12.c show that when the flow is upward  $GR$  is positive. On the other hand when the flow is downward,  $GR$  is negative. It is also clear that analytical and numerical solutions agree very well. This is due to the fact that for  $GR>0$  there is a buoyancy assisted flow and hence flow is upward and for  $GR<0$  there is buoyancy opposed flow and hence flow is downward. We can also observe that the velocity increases with an increase in the value of  $GR$ .A greater energy generated by dissipation forces yields greater fluid temperature which in turn increases the buoyancy force.

The figures 6.2b, 6.7b, 6.12 represent velocity for different values of electric number  $W_e$  and for all the three types of thermal boundary conditions. When temperature difference ( $\Delta T$ ) is in the same direction of potential difference ( $\Delta\phi$ ), We find the electric field is to decrease the velocity with an increase in  $W_e$ . This implies that the effect of electric field is to suppress the convection .On

the other hand, if  $\Delta\phi$  and  $\Delta T$  are in the opposite direction, its augments convection.

Figs 6.2d,6.7d,6.12d gives the velocity for different values of  $Br$ . As  $Br$  increases the velocity also increases and flow reversal occurs for 2<sup>nd</sup> and 3<sup>rd</sup> cases. Figs 6.3a,b,,6.8a,b,6.13a,b, represent the temperature profiles for different values of  $W_e$  and  $T_e$ . In case 1, the increase in  $W_e$  and  $T_e$  increase the heat transfer. In case 2, as  $W_e$  and  $T_e$  increase, the heat transfer also increases.

Figs 6.4a,b, 6.9a,b, 6.14a,b, give the skin friction for different values of  $Br$ . Skin friction decreases linearly through the distance  $y$  and also skin friction decreases with an increase in  $Br$ .

Similarly ,figs 6.5a,b,,6.10a,b,6.15a,b, show that the rate of heat transfer decreases with an increase in  $Br$ . Also figures 6.6a,b,,6.11a,b,6.16a,b, show that the mass flow rate increases with the increase in  $W_e$  and  $Br$  for all the three different thermal boundary conditions. Finally, we conclude that the dissipations enhance the effect of flow reversal in the case of downward flow while it encounter this effect in the case of upward flow.

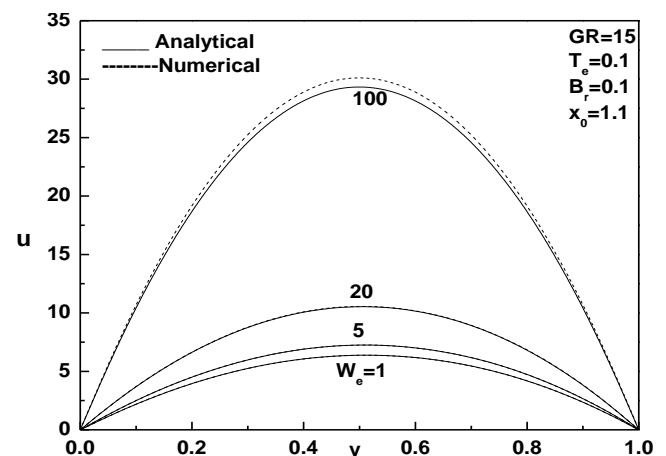


Fig6.2a: Velocity profiles vs electric number  $W_e$  opposite direction, (Isothermal-Isothermal)

Finally we conclude that with a proper choice of external constraints of electric field and the temperature difference it is possible to control MOBEC, which is useful in the manufacture of new materials like smart materials free from impurities.

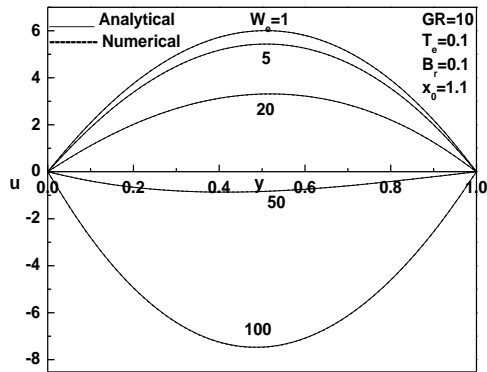


Fig6.2b: Velocity profiles vs electric number  $W_e$  (same direction), (Isothermal-Isothermal)

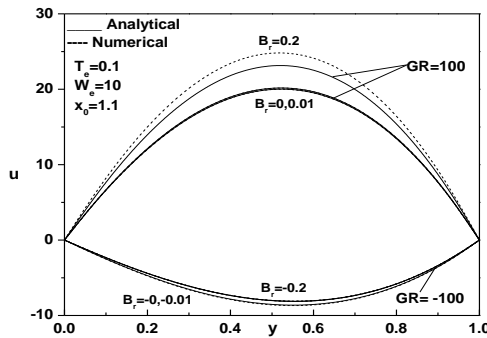


Fig6.2c: Velocity profiles vs  $B_r$  (Isothermal-Isothermal)

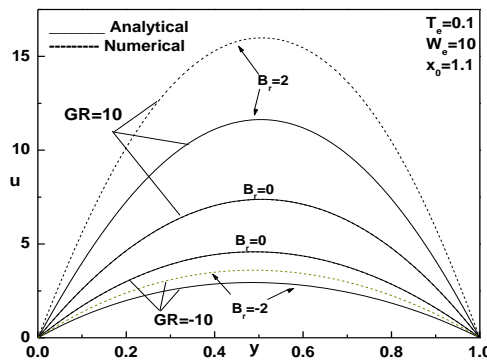


Fig6.2d: Velocity profiles vs  $B_r$  (Isothermal-Isothermal)

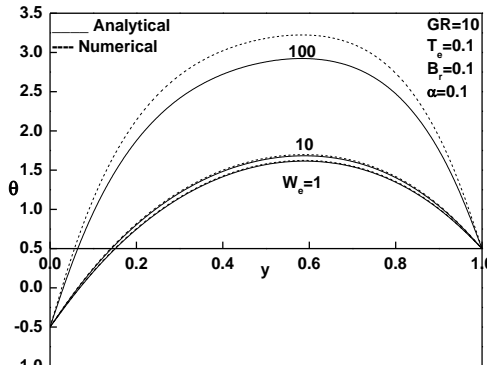


Fig6.3a: Temperature profiles vs  $W_e$  (Isothermal-Isothermal)

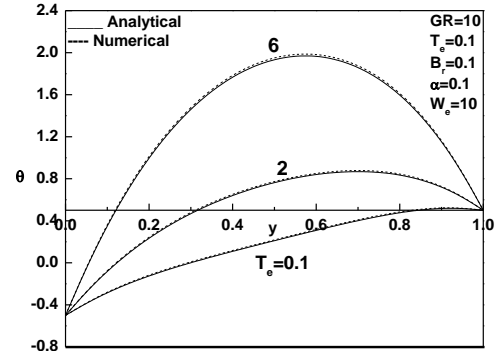


Fig6.3b: Temperature profiles vs  $T_e$  (Isothermal-Isothermal)

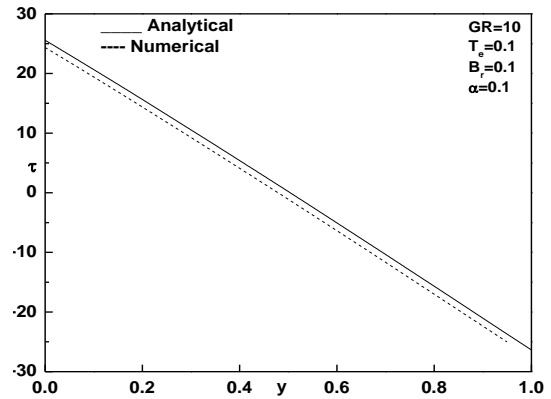


Fig6.4a: Skin friction vs Y with different  $W_e$  (Isothermal-Isothermal)

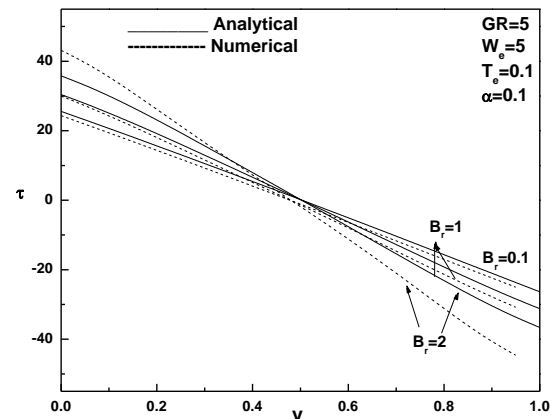


Fig 6.4b: Skin friction vs Y with different  $B_r$  (Isothermal-Isothermal)

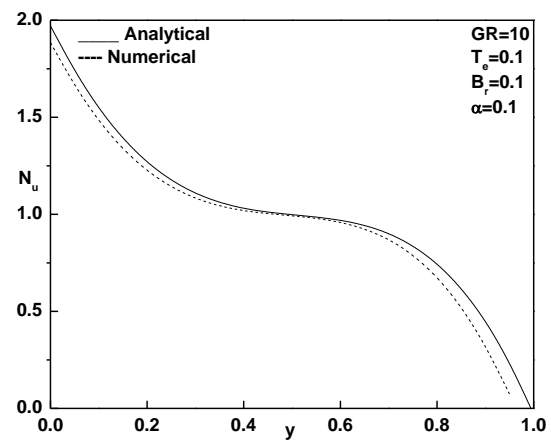


Fig6.5a: Heat transfer vs Y with different  $W_e$  (Isothermal-Isothermal)

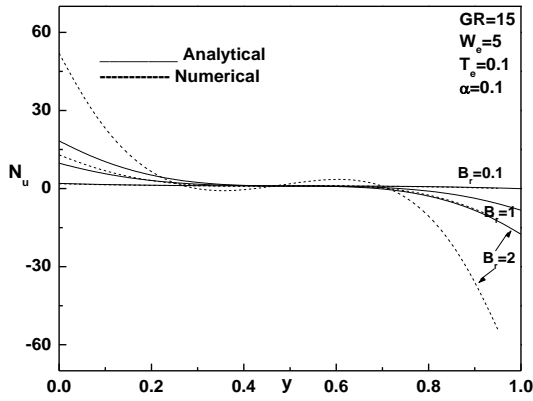


Fig6.5b: Heat transfer with Y with different  $B_r$  (Isothermal-Isothermal)

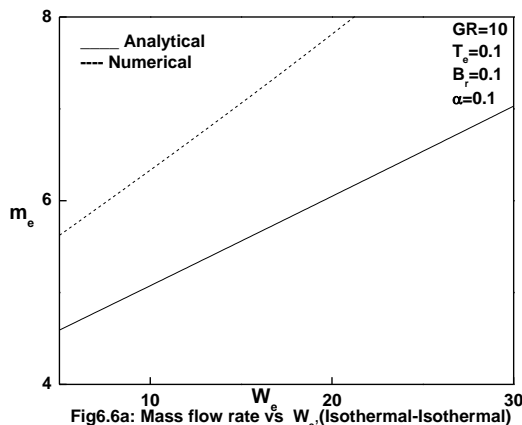


Fig6.6a: Mass flow rate vs  $W_e$  (Isothermal-Isothermal)

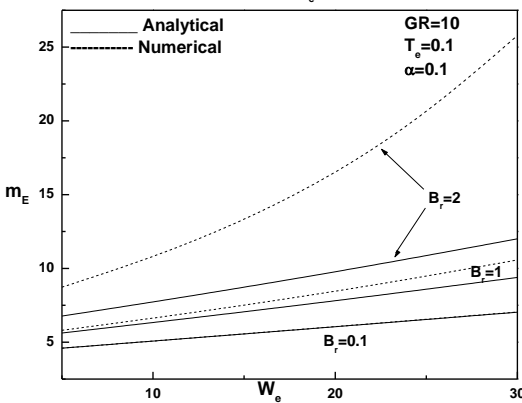


Fig6.6b: Mass flow rate vs  $W_e$  with different  $B_r$  (Isothermal-Isothermal)

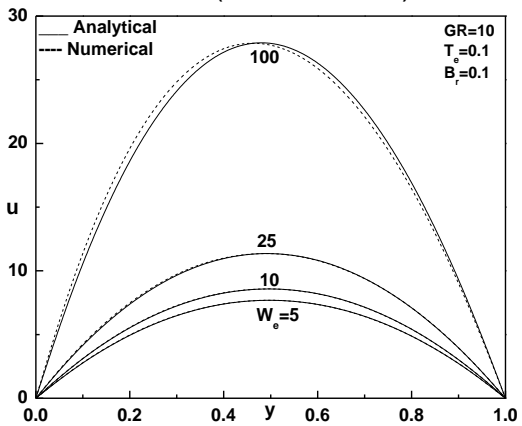


Fig6.7a: Velocity profiles vs Y for different values  $W_e$  (Opposite direction), (Isothermal-Isoflux)

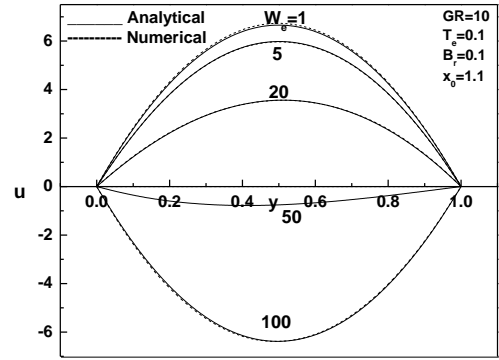


Fig6.7b: Velocity profiles vs Y for different values of  $W_e$  (Same direction), (Isothermal-Isoflux)

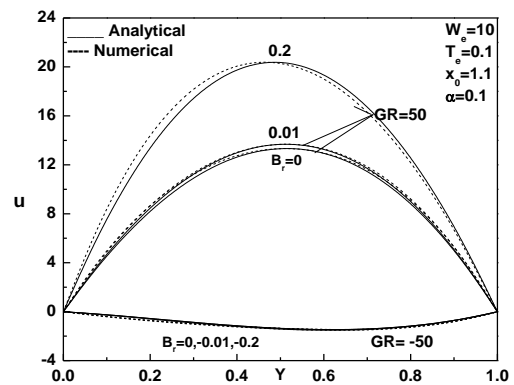


Fig6.7c: Velocity profiles vs Y for different values of  $B_r$  (Isothermal-Isoflux)

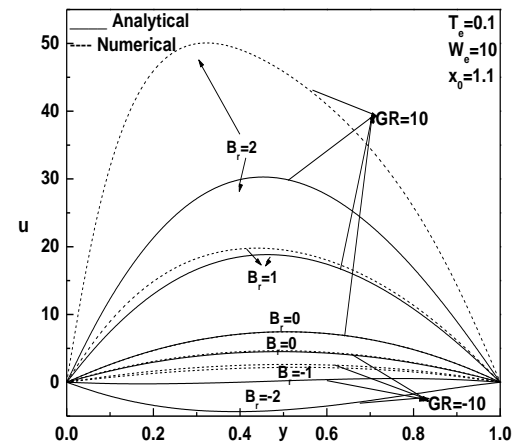


Fig6.7d: Velocity profiles vs Y for different values of  $B_r$  (Isothermal-Isoflux)

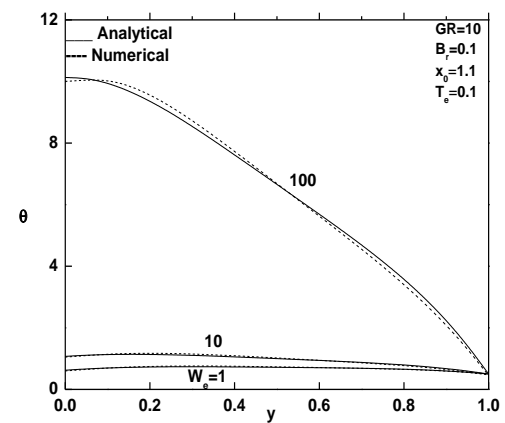


Fig6.8a: Temperature Profile vs Y for different values of  $W_e$  (Isothermal-Isoflux Walls)

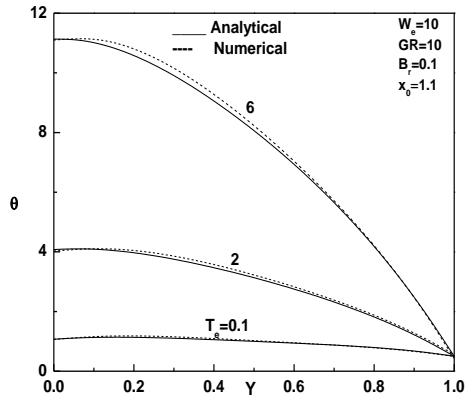


Fig6.8b: Temperature Profile vs Y different values of  $T_0$  (Isothermal-Isoflux Walls)

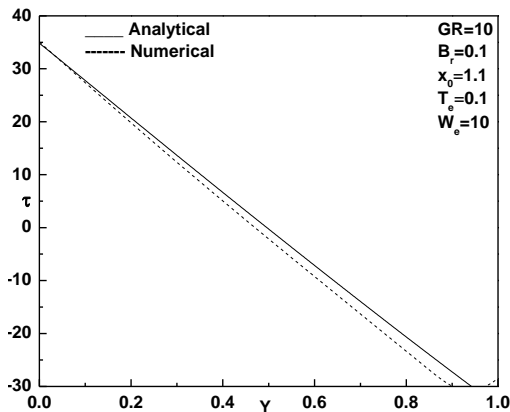


Fig6.9a: Skin friction vs Y (Isothermal-Isoflux Walls)

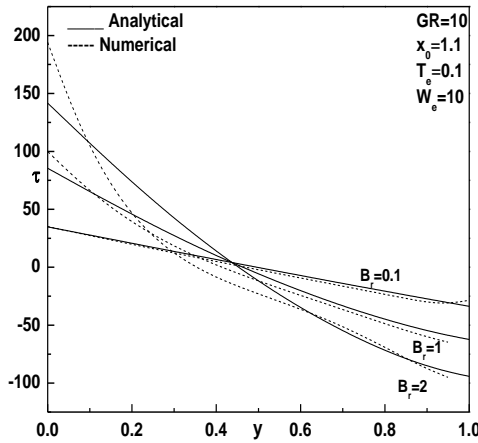


Fig6.9b: Skin friction vs Y for different values of  $B_r$  (Isothermal-Isoflux Walls)

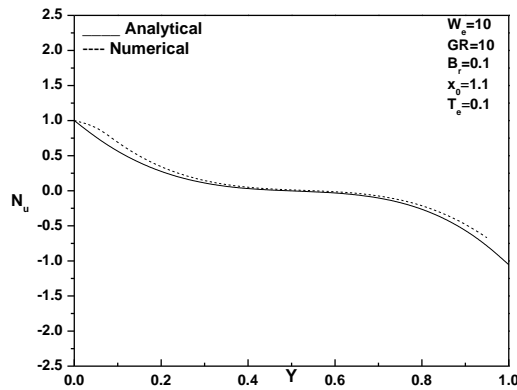


Fig6.10a: Heat transfer vs Y (Isothermal-Isoflux Walls)

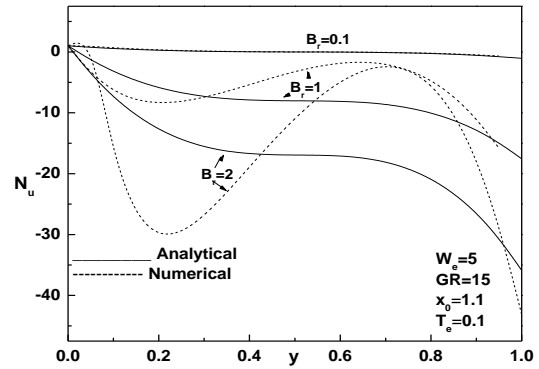


Fig6.10b: Heat transfer vs Y for different values of  $B_r$  (Isothermal-Isoflux Walls)

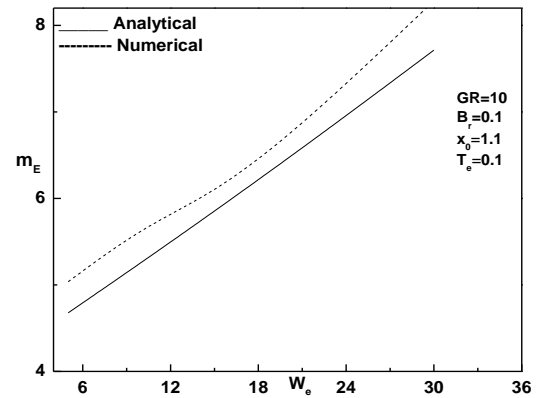


Fig 6.11a: Mass flow rate vs  $W_0$  (Isothermal-Isoflux Walls)

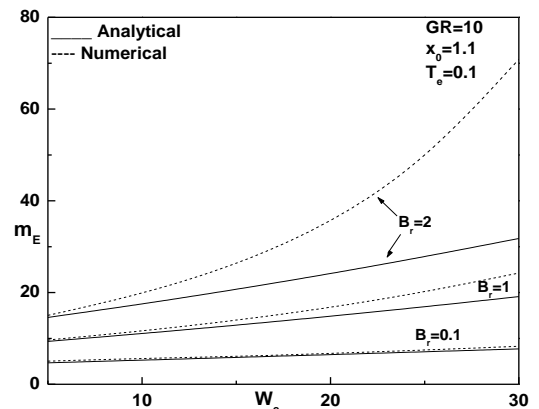


Fig 6.11b: Mass flow rate vs  $W_0$  for different values of  $B_r$  (Isothermal-Isoflux Walls)

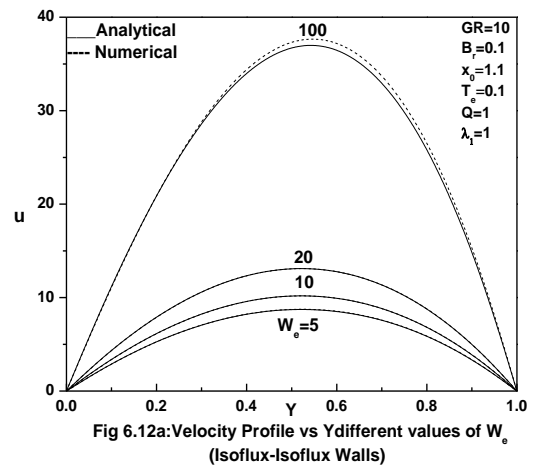


Fig 6.12a: Velocity Profile vs Y different values of  $W_0$  (Isoflux-Isoflux Walls)

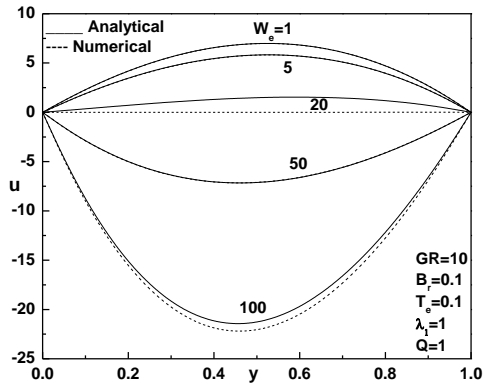


Fig 6.12b: Velocity profiles vs Y for different values of  $W_0$  (Same direction), (Isoflux-Isoflux)

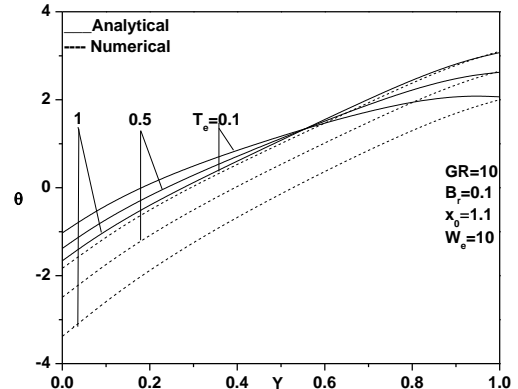


Fig 6.13b: Temperature Profile vs Y for different values of  $T_0$  (Isoflux-Isoflux Walls)

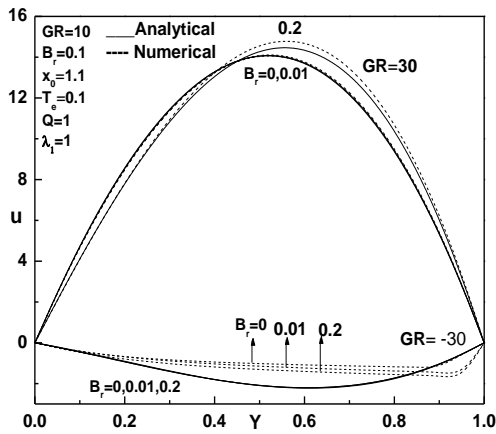


Fig 6.12c: Velocity Profile vs Y different values of  $B_r$  (Isoflux-Isoflux Walls)

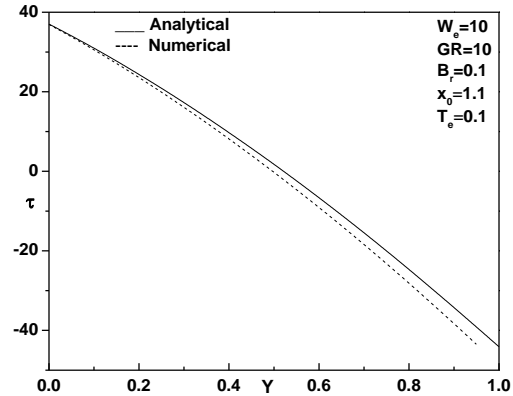


Fig 6.14a: Skin friction vs Y (Isoflux-Isoflux Walls)

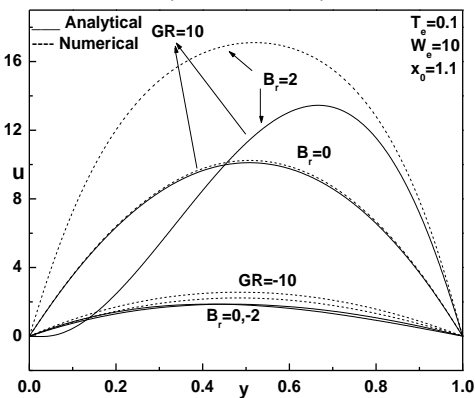


Fig 6.12d: Velocity profiles vs Y for different values of  $B_r$  (Isoflux-Isoflux)

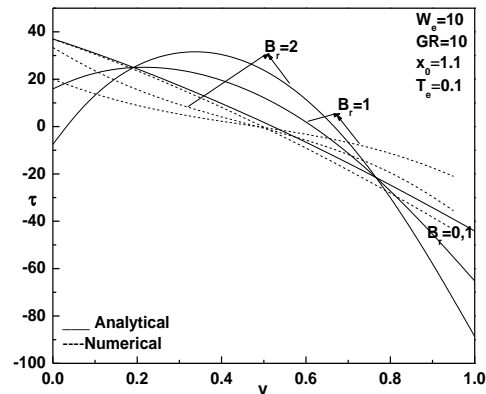


Fig 6.14b: Skin friction vs Y for different values of  $B_r$  (Isoflux-Isoflux Walls)

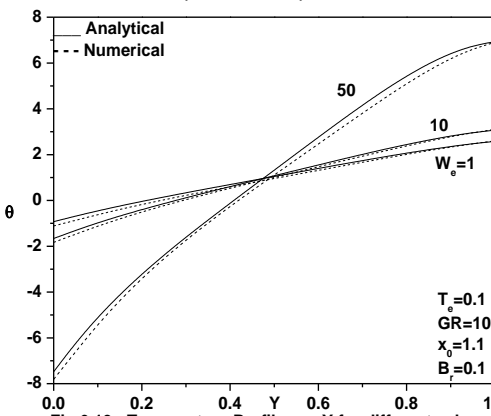


Fig 6.13a: Temperature Profiles vs Y for different values of  $W_0$  (Isoflux-Isoflux Walls)

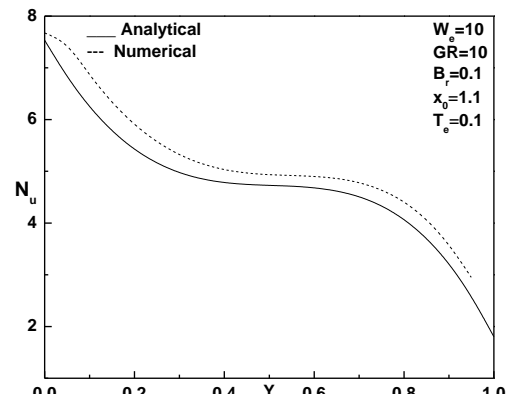
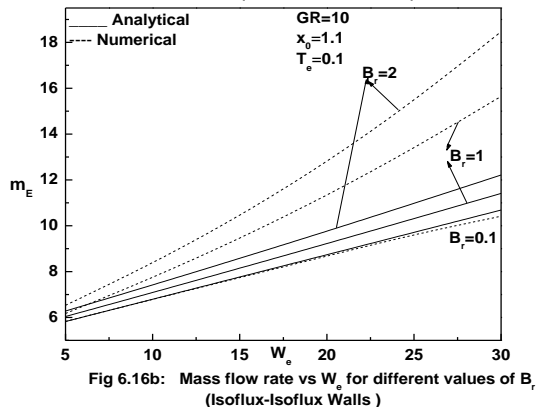
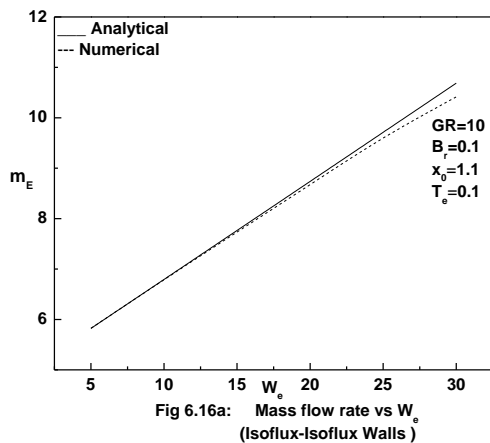
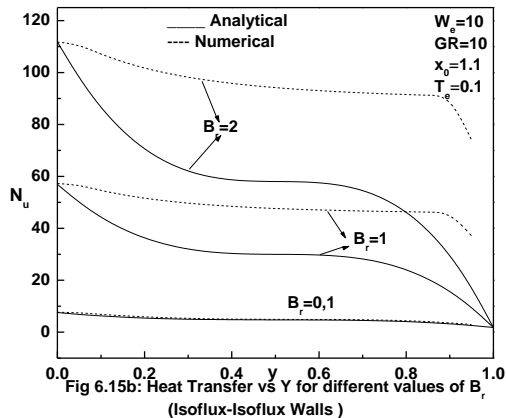


Fig 6.15a: Heat Transfer vs Y (Isoflux-Isoflux Walls)



Note: Because of lack of space we omitted the constants.

### Acknowledgement

The work is supported by TEQIP, Technical education and Principal of GSKSJTI, K.R Circle, Bangalore-01.

### References

W.Aung(Eds)(1987).,Handbook of Single-Phase Convective Heat Transfer, Wiley, New York Chapter 15.

W.M Rohsenow, J.P. Hartnew, Cho.Y.I(1998),Handbook of Heat transfer, McGraw-Hill, New York

L.N .Tao (1960),On combined free and forced convection in channels, ASME J. Heat Transfer , Vol 82,pp.233-23

Win Aung and G .Worku (1987), Mixed convection in ducts with asymmetric wall heat fluxes, ASME J. Heat Transfer , Vol 109,pp.947-951

C.H.Chneg ,H.S.Huang,W.H.Huang(1990),Flow reversal and heat transfer of fully developed mixed convection in vertical channels, J. Thermophys, Heat Transfer, Vol 4, pp.375-383

A. Barlcua (1998), Heat transfer by fully developed flow and viscous heating in a vertical channel with prescribed wall heat fluxes, Int. J. Heat Mass Transfer, Vol 4 ,pp.3501-3513

A. Barlcua (1999), Laminar mixed convection with viscous dissipation in a vertical channel, Int. J. Heat Mass Transfer, Vol 42 ,pp.3873-3885

N. Rudraiah., B.S.Krishnamurhty and R.D.Mathad, (1996), The effect of oblique magnetic field on the surface instability of a finite conducting fluid layer, Acta Mechanica,Vol 119,pp.165

N. Rudraiah. and C.O.Ng, ,(2004), A model for manufacture of Nano-sized smart materials free from impurities, Review Articles, current science, Vol 86 ,No 8,pp. 1076